DNS OF HEAT TRANSFER PHENOMENA IN PLANE TURBULENT WALL JET WITH THERMAL ENTRANCE REGION

H. Hattori
Department of Technical Support, Information and Analysis Technology Division
Nagoya Institute of Technology
Gokiso-cho, Showa-ku, Nagoya 466-855, JAPAN
hattori@nitech.ac.jp

M. Kuroki, T. Houra and M. Tagawa
Department of Electrical and Mechanical Engineering
Nagoya Institute of Technology

ABSTRACT

The objective of this study is to investigate and observe characteristics of heat transfer phenomena in a spatially-developing wall turbulent plane jet by means of direct numerical simulation, where the wall is heated from midstream of field by an isothermal or an isoheat flux boundary conditions, i.e., an entrance region of thermal field is formed. In the velocity field, the maximum mean velocity in the streamwise direction decreases in the downstream region, and Reynolds shear stress in the outer region remarkably increases in comparison with that in the inner region. Thus, the flow situations of inner region is the turbulent boundary layeresque and of outer region is like as the turbulent free shear layer. As for the thermal field, distributions of mean temperature and Nusselt number in the entrance region of thermal field are clearly shown by DNS, in which it is clearly observed that the thermal boundary layer of the isothermal wall condition rapidly develops as compared with that of the isoheat flux wall condition. The different developments by the wall thermal condition of turbulent quantities in thermal field such as the mean temperature, the turbulent heat fluxes and the temperature variance in the plane turbulent wall jet with thermal entrance region are also revealed.

INTRODUCTION

A wall turbulent plane jet is a shear flow which has both the boundary layer in the inner layer and the free shear layer in the outer layer. Also, a wall turbulent plane jet is used for the cooling of surface of solid. Thus, it is important that the characteristics, structures and mechanism of both flow and heat transfer phenomena are investigated and observed in detail in order to improve the performance of heat transfer. As for the wall jet, it is well-known that the wall jet is divided by the potential core region which does not decrease the maximum velocity and the development region which is formed by the mixture of inner and outer shear layers (Myers *et al.*, 1963; Herbst & Sforza, 1970). Thus, the characteristics of heat transfer phenomena may also vary in both the regions. On the other hand, the turbulent heat transfer phenomena in various turbulent boundary layers have been studied using the direct numerical simulation (DNS) in detail (Hattori & Nagano, 2004; Hattori *et al.*, 2007, 2013, 2014). Since the turbulent statistics of both velocity and thermal fields including the data in the vicinity of the wall which are hardly measured by the experiment can be obtained by the DNS, the characteristics, structures and mechanism of both flow and heat transfer phenomena in various turbulent flows have been revealed(Hattori & Nagano, 2004; Hattori *et al.*, 2007, 2013, 2014). In order to more find out heat transfer phenomena in wall shear flows, an investigation and an observation of characteristics, structures and mechanism of a wall turbulent plane jet are required using DNS.

In this study, in order to investigate and observe heat transfer phenomena in a wall turbulent plane jet, DNS of a spatially-developing wall turbulent plane jet with heat transfer is carried out where the wall is heated from midstream of field by an isothermal or an isoheat flux boundary conditions, i.e., an entrance region of thermal field is formed. In DNS, the characteristics, structures and mechanism of turbulent heat transfer in wall turbulent plane jet are revealed.

DNS OF SPATIALLY-DEVELOPING WALL TURBULENT PLANE JET WITH THERMAL ENTRANCE REGION

The governing equations used in the present DNS are indicated as follows (Hattori & Nagano, 2004):

$$\frac{\partial u_i}{\partial t}+u_j\frac{\partial u_i}{\partial x_j}=-\frac{\partial p}{\partial x_i}+\frac{1}{Re_D}\frac{\partial^2 u_i}{\partial x_j\partial x_j} \tag{1}$$

$$\frac{\partial u_i}{\partial x_i}=0 \tag{2}$$

$$\frac{\partial \theta}{\partial t}+u_j\frac{\partial \theta}{\partial x_j}=\frac{1}{Pr\,Re_D}\frac{\partial^2 \theta}{\partial x_j\partial x_j} \tag{3}$$

where the Einstein summation convention applies to repeated indices, u_i is the dimensionless velocity component in x_i direction, θ is the dimensionless temperature, p is the dimensionless pressure, t is the dimensionless time, and x_i is the dimensionless spatial coordinate in the i direction, respectively. $Re_D=\bar{U}_bD/\nu(=5670)$ is the Reynolds number

based on the bulk velocity and the height of inlet channel which is the driver part. Note that "the driver part" means the inflow data generator for the inlet boundary of the main simulation part as shown in Fig. 1. $Pr = \nu/\alpha (= 0.71)$ is the Prandtl number. In the governing equations, the dimensionless variables are given using the bulk velocity of the inlet channel, U_b, the half width of inlet channel, the temperature difference between inlet and wall temperature, $\Delta\Theta$, for the case of isothermal wall, and the corrected temperature using the wall heat flux, $q_w D/\lambda$, for the case of isoflux wall.

For efficiently conducting the DNS of a spatially-developing wall turbulent plane jet with heat transfer, the computational domain is composed of two parts; one is the driver part where a fully-developing turbulent channel flow with an adiabatic wall is generated and used as the inflow boundary condition for the main simulation, and the other is the main part where a spatially-developing wall turbulent plane jet with heat transfer are simulated. A central finite-difference method of second-order accuracy is used to solve the equations of continuity, momentum and energy (Hattori & Nagano, 2004; Hattori *et al.*, 2007), where the computational domain is arranged as $x \times y \times z = 20.5D \times 30D \times 1.6D$. The grid points are given as $x \times y \times z = 820 \times 352 \times 128$ in the main simulation part, and $x \times y \times z = 128 \times 96 \times 128$ in the driver part. The resultant spatial resolutions by the wall unit of the main simulation part are $\Delta x^+ = 8 \sim 9$, $\Delta y^+ = 0.36 \sim 12$, and $\Delta_z^+ = 4 \sim 4.5$, respectively.

The non-slip condition for velocity field and the isothermal or the isoflux conditions for thermal field at the wall, and the convective boundary condition (Hattori *et al.*, 2007) at the outlet, the free slip condition at the upper side, and the periodic condition for the spanwise direction are adopted for both velocity and thermal fields.

RESULTS AND DISCUSSION

Figure 2 shows the distribution of modified wall friction coefficient, $C_f Re_D^{1/4}$, along the wall, in which the empirical relations in the fully developed turbulent flow (Blasius, 1913; Dean, 1978) are included. In the wall jet, it was reported that the wall friction coefficient is proportional to $C_f \propto C Re_D^n (x/D)^m$ (Myers *et al.*, 1963), where C is the proportionality constant. The behavior of modified wall friction coefficient in the core region almost agrees with Blasius's law, $C_f Re_D^{1/4} = 0.0664$, up to about $x/D = 3$, and then the modified wall friction coefficient slowly decreases in the transition region as indicated in Fig. 2. Finally, the behavior in the wall jet developing region becomes $C_f Re_D^{1/4} = 0.11(x/D)^{-1/4}$ from the vicinity of $x/D = 10$.

The profiles of streamwise mean velocity normalized by both outer and inner scales are shown in Fig 3. Since the maximum velocity hardly decreases near $x/D = 3$, it

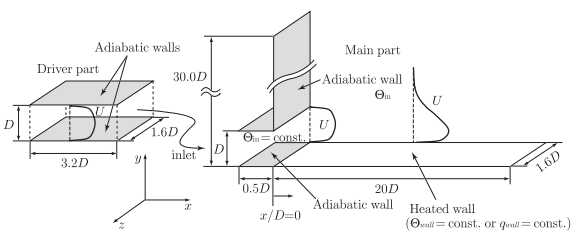

Figure 1. Schematic and domain of flow field

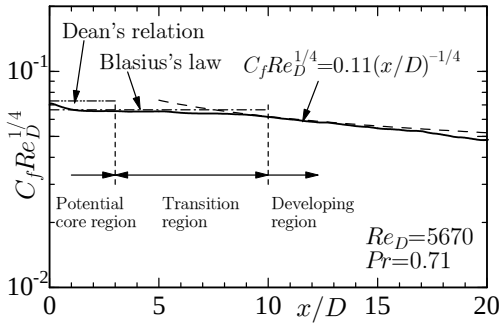

Figure 2. Wall friction coefficient

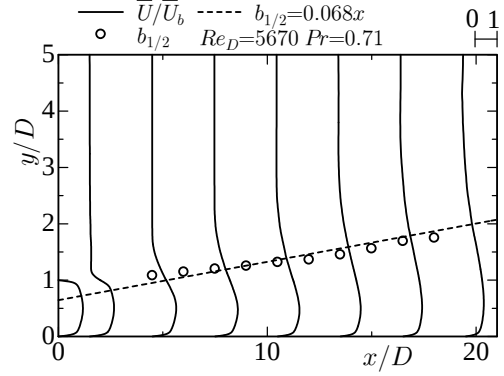

(a) Normarized by outer scale

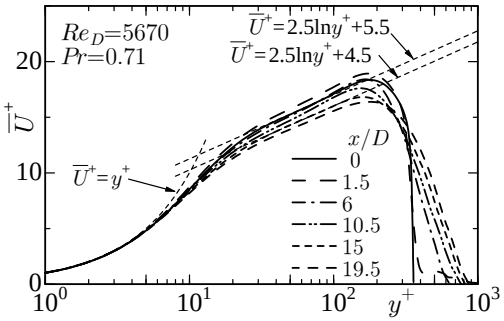

(b) Normarized by inner scale

Figure 3. Profiles of streamwise mean velocities

is found that the potential core region exists by this point as mentioned above. The expansion of half width, $b_{1/2}$, of streamwise mean velocity agrees with the relation obtained by experiment $b_{1/2}/D = 0.068(x/D)$ (Rajaratnam, 1976) whose the origin is $x/D = -10$. As for the streamwise mean velocity normalized by inner scale, variations of profile can be observed in the log region, i.e., the profile fits the log-law of $\bar{U}^+ = 2.5 \ln y^+ + 5.5$ in the core region, but the profile fits the log-law of $\bar{U}^+ = 2.5 \ln y^+ + 4.5$ in the developing region as shown in Fig. 3(b). Distributions of Reynolds shear stress are shown in Fig. 4, in which the expansion of distribution of Reynolds shear stress in the downstream region can be observed. In the view of the inner scale normalization as shown in Fig. 4(b), a few changes in the inner region and remarkable variations in the outer region of Reynolds shear stresses are also observed. Thus, the flow situations of inner region is the turbulent boundary layeresque and of outer region is like as the turbulent free shear layer. In Figs. 5$\sim$ 7, distributions of turbulent kinetic energy and rms velocity fluctuations are indicated, where

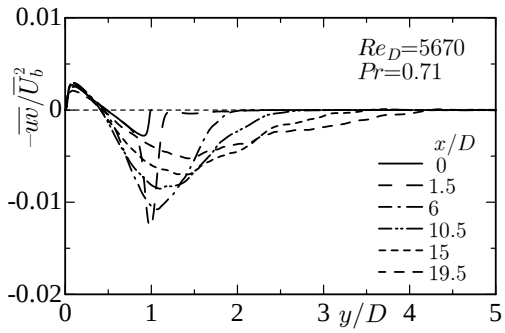

(a) Normarized by outer scale

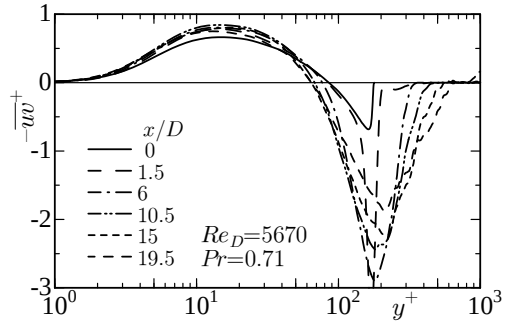

(b) Normarized by inner scale

Figure 4. Distributions of Reynolds shear stresses

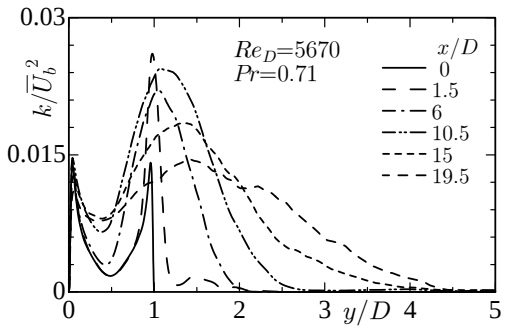

(a) Normarized by outer scale

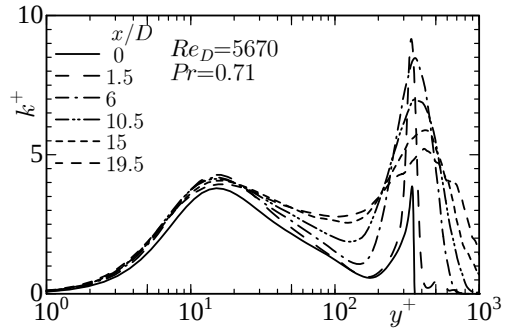

(b) Normarized by inner scale

Figure 5. Distributions of turbulent kinetic energy

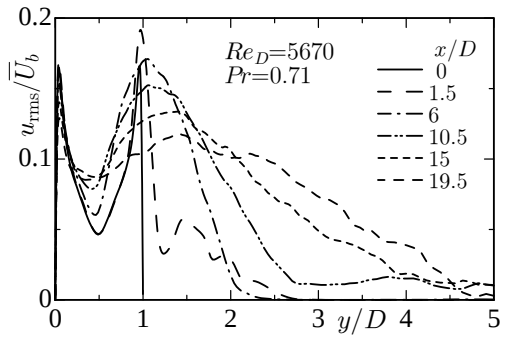

(a) Normarized by outer scale

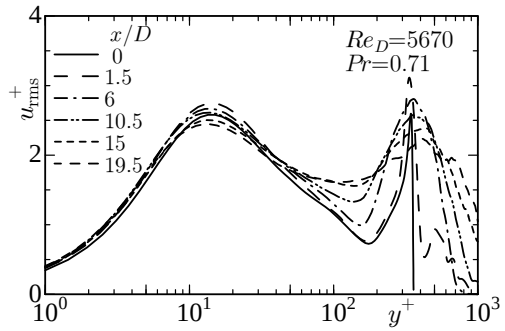

(b) Normarized by inner scale

Figure 6. Distributions of streamwise rms velocity fluctuations

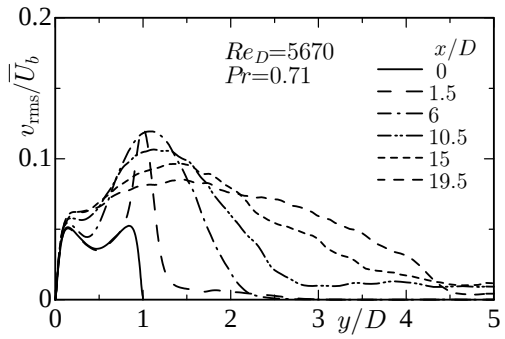

(a) Normarized by outer scale

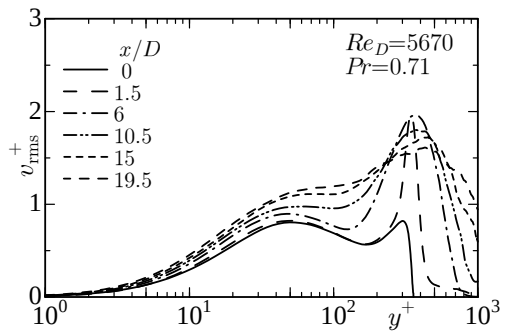

(b) Normarized by inner scale

Figure 7. Distributions of wall-normal rms velocity fluctuations

remarkable variations of turbulent kinetic energy and rms velocity fluctuations in the outer region are observed, but it can be seen that the wall-normal rms velocity fluctuation also increases in the inner region. Thus, it is obvious that the turbulent motion toward to the wall-normal direction is very enhanced. Therefore, the vortex structure also expands in the downstream region as shown in Fig. 8, where development of both the vortex structures in the boundary layer and in the free shear layer can be clearly observed, and then the mixture of vortex structures in the downstream region

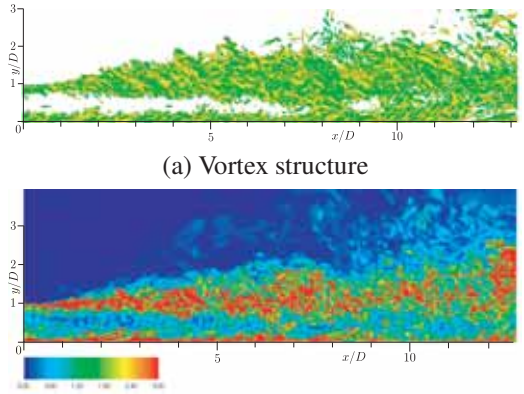

(a) Vortex structure

(b) Magnitude of vorticity

Figure 8. Vortex structure and magnitude of vorticity

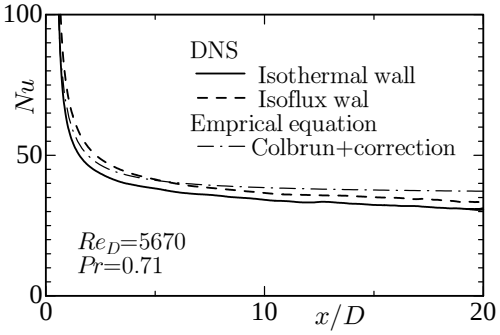

Figure 9. Local Nusselt numbers in both wall thermal conditions

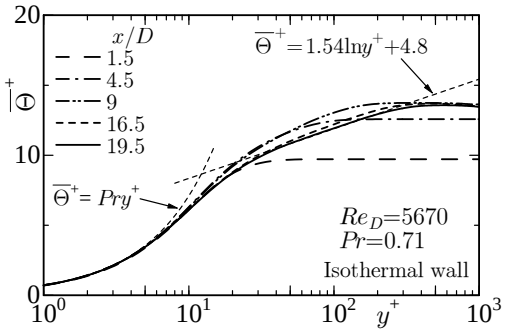

(a) Isothermal wall condition

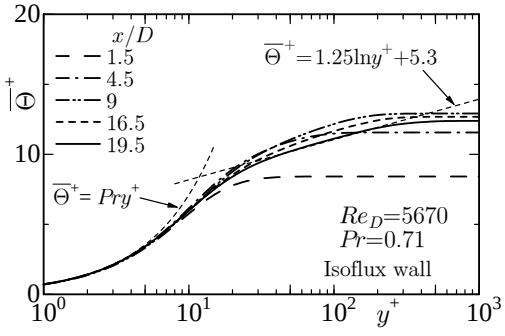

(b) Isoflux wall condition

Figure 10. Profiles of mean temperature

are found. Figure 8 also shows the magnitude of vorticity,

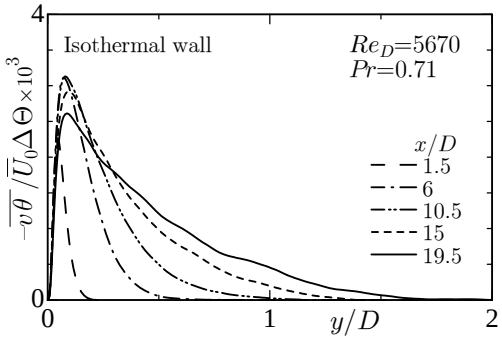

(a) Normarized by outer scale

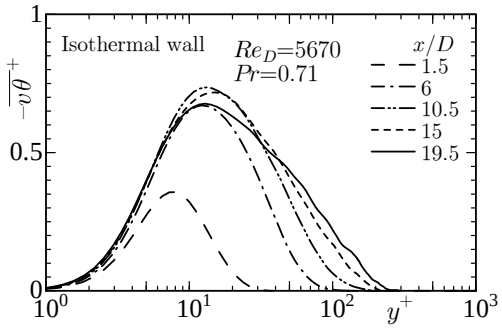

(b) Normarized by inner scale

Figure 11. Distributions of wall-normal turbulent heat flux (Isothermal wall condition)

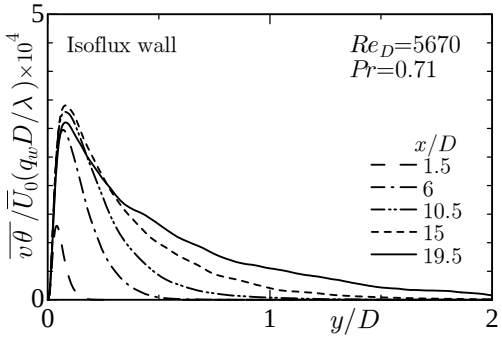

(a) Normarized by outer scale

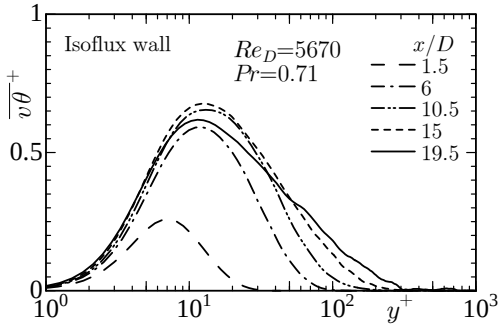

(b) Normarized by inner scale

Figure 12. Distributions of wall-normal turbulent heat flux (Isoflux wall condition)

$|\Omega|$, calculated by $|\Omega| = \sqrt{\Omega_i \Omega_i}$, where the irrotational region can be clearly observed in the outer region, i.e., the entrainment phenomenon appears.

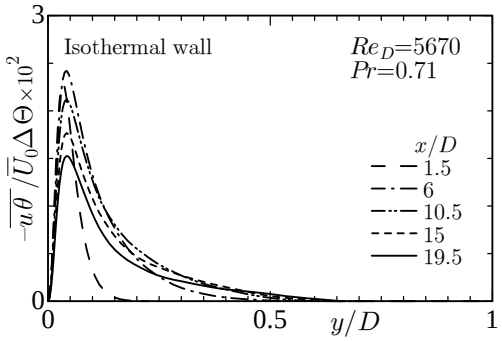

(a) Normarized by outer scale

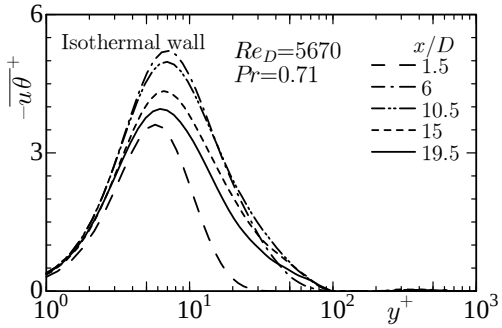

(b) Normarized by inner scale

Figure 13. Distributions of streamwise turbulent heat flux (Isothermal wall condition)

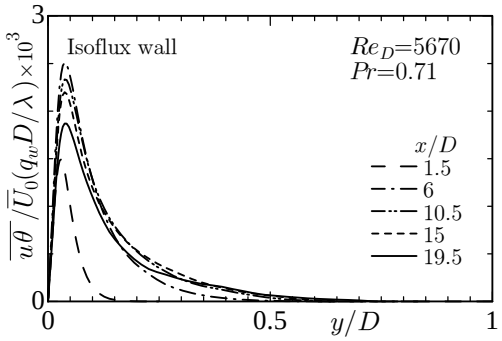

(a) Normarized by outer scale

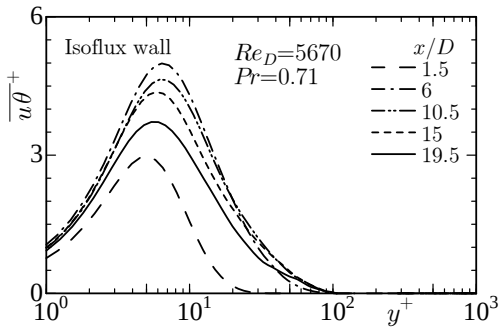

(b) Normarized by inner scale

Figure 14. Distributions of streamwise turbulent heat flux (Isoflux wall condition)

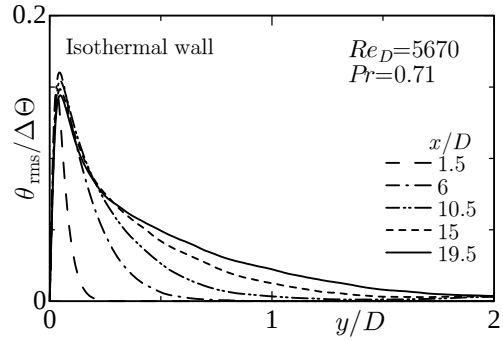

(a) Normarized by outer scale

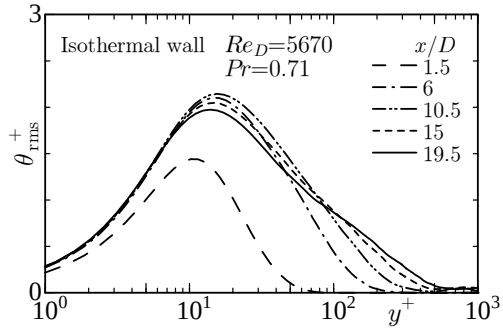

(b) Normarized by inner scale

Figure 15. Distributions of rms temperature fluctuations (Isothermal wall condition)

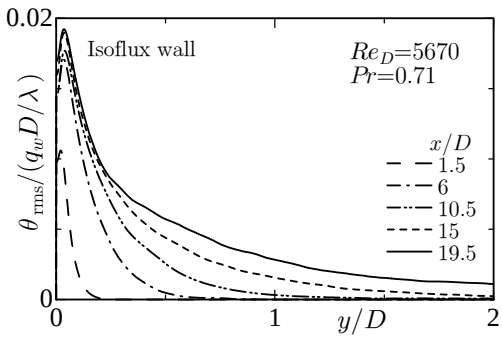

(a) Normarized by outer scale

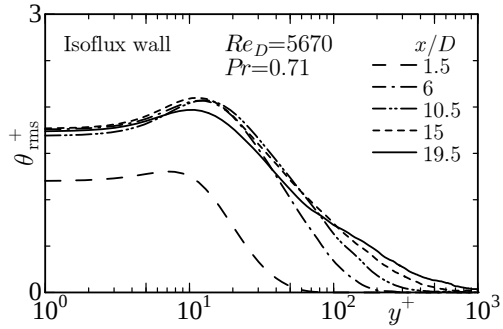

(b) Normarized by inner scale

Figure 16. Distributions of rms temperature fluctuations (Isoflux wall condition)

The distribution of Nusselt numbers, $Nu = 2hD/\lambda$, is shown in Fig. 9 in which the empirical relation with correction for thermal entrance region is included (Colburn, 1933; McAdams, 1954). Due to the entrance region of thermal field, the maximum Nusselt numbers is given at the start point of heating, in which Nusselt number of the case of

isothermal wall rapidly decreases than that of the case of isoflux wall. From observation of distributions of Nusselt numbers, influence of the wall jet is hardly found, i.e., the distributions are similar with these of entrance region in turbulent boundary layer.

Figure 10 shows profiles of mean temperature normalized by inner scale. The development of mean temperature in the entrance region can be clearly observed in both the cases, in which the profiles of mean temperature in the log-law region of developing region fit the function of $\bar{\Theta}^+ = 1.54 \ln y^+ + 4.8$ for the isothermal condition and of $\bar{\Theta}^+ = 1.25 \ln y^+ + 5.3$ for the isoflux condition, respectively. The distributions of wall-normal and streamwise turbulent heat fluxes in both wall conditions are shown in Figs. 11$\sim$ 14. Developments of both turbulent heat fluxes can be obviously found in both cases due to the entrance region of thermal field. Observing the profiles of wall-normal turbulent heat flux normalized by outer scale of both cases as shown in Figs 11(a) and 12(a), it reveals that the development of thermal field in the case of isothermal wall is faster than that in the case of isoflux wall, but the wall-normal turbulent heat flux in case of isoflux condition in the developing region widely distributes in comparison with the distribution of the wall-normal turbulent heat flux in case of isothermal condition. As for the streamwise turbulent heat flux as shown in Figs. 13 and 14, the development is also observed similar with the distribution of wall-normal turbulent heat flux, but it can be seen that the distributed region of streamwise turbulent heat flux of both cases are restricted in comparison with distributed region of wall-normal turbulent heat flux. This is because it is considered that the streamwise rms velocity does not very change in the inner region. The development situations of streamwise turbulent heat flux in both cases are very similar, where it can be seen that the maximum values once increase in the transition region, and then the values decreases in the developing region. Distributions of rms temperature fluctuations in both cases are shown in Figs. 15 and 16. It is clearly observed that rms temperature fluctuations of both cases develops toward the outer region, but uniform distributions normalized by the inner scale can be seen except for the distribution in the core region. Also, the near-wall different distributions of rms temperature fluctuation can be observed due to the boundary condition at the wall, i.e., rms temperature fluctuation has a value at the wall in the isoflux wall condition (Hattori *et al.*, 2013). Therefore, the different developments of rms temperature fluctuations occur as shown in Figs. 15(a) and 16(a).

CONCLUSIONS

In order to investigate and observe characteristics of heat transfer phenomena in a spatially-developing wall turbulent plane jet by means of direct numerical simulation, where the wall is heated from midstream of field by an isothermal or an isoheat flux boundary conditions, i.e., an entrance region of thermal field is formed. In the velocity field, variations of the modified friction coefficient are clearly observed due to variations of flow situation, i.e., the potential core region, the transition region and the developing region exist. The maximum mean velocity in the streamwise direction decreases in the downstream region, and Reynolds shear stress in the outer region remarkably increases in comparison with that in the inner region. Thus, the flow situations of inner region is the turbulent boundary layeresque and of outer region is like as the turbulent free shear layer. Especially, it is observed that the wall-normal rms velocity fluctuation is enhanced in both the inner and outer regions. It can be seen that the vortex structures are developing along the wall and in the turbulent free shear layer, and the mixture of these structures in the downstream region can be observed. As for the thermal field, distributions of mean temperature and Nusselt number in the entrance region of thermal field are clearly shown by DNS, in which it is clearly observed that the thermal boundary layer of the isothermal wall condition rapidly develops as compared with that of the isoheat flux wall condition. Developments of both wall-normal and streamwise turbulent heat fluxes in the entrance region of thermal field are also revealed, where it can be seen that the distributed region of streamwise turbulent heat flux of both cases are restricted in comparison with distributed region of wall-normal turbulent heat flux due to hardly changing the streamwise rms velocity in the inner region. Also, the occurrence of different developments of rms temperature fluctuation due to the wall thermal conditions are revealed.

ACKNOWLEDGEMENTS

This work was supported by JSPS KAKENHI Grant Numbers JP26420144 and JP26420143 and by Cross-ministerial Strategic Innovation Promotion Program (SIP), "Innovative Combustion Technology" (funding agency: Japan Science and Technology Agency, JST).

REFERENCES

Blasius, H. 1913 Das ähnlichkeitsgesetz bei reibungsvorgängen in flüssigkeiten. *Forschg. Arb. Ing.-Wes.* (134).

Colburn, A.P. 1933 A method of correlating forced convection heat transfer data and a comparison with fluid friction. *Trans. AIChE* **29**, 174–210.

Dean, R.B. 1978 Reynolds number dependence of skin friction and other bulk flow variables in two-dimensional rectangular duct flow. *ASME. Journal of Fluids Engineering* **100**, 215–223.

Hattori, H., Hotta, K. & Houra, T. 2014 Characteristics and structures in thermally-stratified turbulent boundary layer with counter diffusion gradient phenomenon. *International Journal of Heat and Fluid Flow* **49**, 53 – 61.

Hattori, H., Houra, T. & Nagano, Y. 2007 Direct numerical simulation of stable and unstable turbulent thermal boundary layers. *International Journal of Heat and Fluid Flow* **28**, 1262–1271.

Hattori, H & Nagano, Y 2004 Direct Numerical Simulation of Turbulent Heat Transfer in Plane Impinging Jet. *International Journal of Heat and Fluid Flow* **25**, 749–758.

Hattori, H., Yamada, S., Tanaka, M., Houra, T. & Nagano, Y. 2013 DNS , LES and RANS of turbulent heat transfer in boundary layer with suddenly changing wall thermal conditions. *International Journal of Heat and Fluid Flow* **41**, 34–44.

Herbst, G. & Sforza, P.M. 1970 A study of three-dimensional, incompressible, turbulent wall jets. *AIAA Journal* **8** (2), 276–283.

McAdams, W.H. 1954 *Heat Transmission 3rd ed.*. McGraw-Hill.

Myers, G.E., Schauer, J.J. & Eustis, R.H. 1963 Plane turbulent wall jet flow development and friction factor. *ASME. Journal of Basic Engineering* **85**, 47–53.

Rajaratnam, N. 1976 *Turbulent jets*, , vol. 5. Elsevier.